Unimolecular Electrical Rectification in Hexadecylquinolinium Tricyanoquinodimethanide

Robert M. Metzger,*,† Bo Chen,† Ulf Höpfner,†,‖ M. V. Lakshmikantham,† Dominique Vuillaume,†,⊥ Tsuyoshi Kawai,†,# Xiangli Wu,† Hiroaki Tachibana,†,▽ Terry V. Hughes,† Hiromi Sakurai,† Jeffrey W. Baldwin,† Christina Hosch,†,○ Michael P. Cava,† Ludwig Brehmer,‡ and Geoffrey J. Ashwell§

Contribution from the Laboratory for Molecular Electronics, Chemistry Department, University of Alabama, Tuscaloosa, Alabama 35487-0336, Solid State Physics Institute, University of Potsdam, Am Neuen Palais 10, D-14469 Potsdam, Germany, and Centre for Molecular Electronics, Cranfield University, Cranfield, Bedfordshire MK43 0AL, United Kingdom

Received June 2, 1997[⊗]

Abstract: Macroscopic and nanoscopic current−voltage measurements reveal asymmetries in the DC electrical conductivity through Langmuir−Blodgett multilayers and even monolayers of γ-(*n*-hexadecyl)quinolinum tricyanoquinodimethanide, $C_{16}H_{33}$Q-3CNQ (**5**). These asymmetries are due to a transition of the ground-state zwitterion to an excited-state conformer which is probably neutral. Unimolecular electrical rectification by monolayers of **5** is unequivocally confirmed.

1. Introduction

Molecular rectification of electrical current can be defined as a strongly asymmetric flow of electrons through a molecule because the conductivity from, say, the left "side" of the molecule to its right "side" is very different from the conductivity from "right" to "left".

Rectification of electrical current was first achieved almost a century ago in vacuum diodes,[1] then later in junctions of p-doped Ge accosted to n-doped Ge.[2] For inorganic semiconductors, rectification will occur either (i) at an interface, whenever a "Schottky barrier" is formed at the boundary between phases with dissimilar work functions,[3] or (ii) within a much wider "depletion layer", when the charge compensation between differently doped regions extends several micrometers within the semiconductor.[2]

Rectification by junctions of micrometer-thick layers of n-doped organic semiconductors with micrometer-thick layers of p-doped organic semiconductors is well-known.[4−7]

Electrical rectification by Langmuir−Blodgett multilayers (doped with electron donors (D), topped by insulating LB monolayers, then topped by multilayers "doped" with electron acceptors (A)) was demonstrated by Kuhn and co-workers[8] and confirmed by other groups.[9,10] An electrochemical Langmuir−Blodgett photodiode was produced by Fujihira;[11] electrochemical rectification at a monolayer-modified electrode has been reported.[12,13] Aviram, Pomerantz, and co-workers attached a porphyrin covalently to a carboxylated highly oriented pyrolytic graphite (HOPG) surface and studied it by scanning tunneling microscopy (STM).[14] An unsymmetrical STM tunneling current was also seen through an alkylated hexabenzocoronene deposited on graphite[15] (this may be due to some salt formation?) and an oligophenylethynyl)benzenethiol on Au(111) and Ag-(111).[16]

A major challenge has been to provide experimental verification of the Aviram−Ratner (AR) ansatz[17] of unimolecular rectification, or asymmetrical electrical conduction, through the molecular orbitals of a single D−σ−A molecule ("through-bond tunneling"). Here D = good one-electron donor with low ionization potential, A = good electron acceptor with high electron affinity, and σ = insulating saturated covalent "bridge".[17] This unimolecular rectification would work because the excited zwitterionic state $D^+-\sigma-A^-$ would be relatively accessible from the ground neutral state D−σ−A, while the opposite

* Author to whom correspondence should be addressed.
† University of Alabama.
‡ University of Potsdam.
§ Cranfield University.
‖ Present address: Solid State Physics Institute, University of Potsdam, Am Neuen Palais 10, D-14469 Potsdam, Germany.
⊥ Permanent address: Institut d'Électronique et de Microélectronique du Nord, CNRS, P.O. Box 69, Avenue Poincaré, F-59652 Villeneuve d'Ascq cedex, France.
Permanent address: Department of Electronic Engineering, Osaka University, 2-1 Yamada-oka, Suita, Osaka 565, Japan.
▽ Present address: National Institute of Materials and Chemical Research, 1-1 Higashi, Tsukuba, Ibaraki 305, Japan.
○ National Science Foundation Summer Research Employment for Undergraduates Participant from Clarke College, Dubuque, IA.
⊗ Abstract published in *Advance ACS Abstracts,* October 1, 1997.

(1) Fleming, J. A. U. K. Patent 24,850 (appl. Nov. 16, 1904); U.S. Patent 803,684 (granted Apr. 19, 1905).
(2) Shockley, W. *Bell System Technol. J.* **1949**, *28*, 435−489.
(3) Schottky, W. *Z. Phys.* **1942**, *118*, 539−592.
(4) Meinhard, J. E. *J. Appl. Phys.* **1964**, *35*, 3059−3060.
(5) Anderson, T. L.; Komplin, G. C.; Pietro, W. J. *J. Phys. Chem.* **1993**, *97*, 6577−6578.
(6) Pietro, W. J. *Adv. Mater.* **1994**, *6*, 239−242.
(7) Hamm, S.; Wachtel, H. *J. Chem. Phys.* **1994**, *103*, 10689−10695.
(8) Polymeropoulos, E. E.; Möbius, D.; Kuhn, H. *Thin Solid Films* **1980**, *68*, 173−190.
(9) Sugi, M.; Sakai, K.; Saito, M.; Kawabata, Y.; Iizima, S. *Thin Solid Films* **1985**, *132*, 69−76.
(10) Fischer, C. M.; Burghard, M.; Roth, S.; v. Klitzing, K. *Europhys. Lett.* **1994**, *28*, 129−134.
(11) Fujihira, M.; Nishiyama, K.; Yamada, H. *Thin Solid Films* **1986**, *132*, 77−82.
(12) Sato, Y.; Itoigawa, H.; Uosaki, K. *Bull. Chem. Soc. Jpn.* **1993**, *66*, 1032−1037.
(13) Alleman, K. S.; Weber, K.; Creager, S. E. *J. Phys. Chem.* **1996**, *100*, 17050−17058.
(14) Pomerantz, M.; Aviram, A.; McCorkle, R. A.; Li, L.; Aschott, A. G. *Science* **1992**, *255*, 1115−1118.
(15) Stabel, A.; Herwig, P.; Müllen, K.; Rabe, J. P. *Angew. Chem., Int. Ed. Engl.* **1994**, *34*, 1609−1611.
(16) Dhirani, A.; Lin, P.-H.; Guyot-Sionnest, P.; Zehner, R. W.; Sita, L. R. *J. Chem. Phys.* **1997**, *106*, 5249−5253.
(17) Aviram, A.; Ratner, M. A. *Chem. Phys. Lett.* **1974**, *29*, 277−283.

S0002-7863(97)01811-8 CCC: $14.00

zwitterion $D^-{-}\sigma{-}A^+$ would lie several electronvolts higher in energy and, therefore, be inaccessible, except at dielectric breakdown: good organic one-electron donors (e.g., tetrathiafulvalene, TTF, **1**) are poor acceptors, while good acceptors (e.g., tetracyanoquinodimethane, TCNQ, **2**) are very poor one-electron donors:

$$D{-}\sigma{-}A \rightarrow D^+{-}\sigma{-}A^- + (1{-}2\ \text{eV}) \quad (1)$$

$$D{-}\sigma{-}A \rightarrow D^-{-}\sigma{-}A^+ + (9\ \text{eV}) \quad (2)$$

Several such $D{-}\sigma{-}A$ molecules suitable for LB film formation were prepared and studied by simple methods, but evidence of rectification was not found.[18−20]

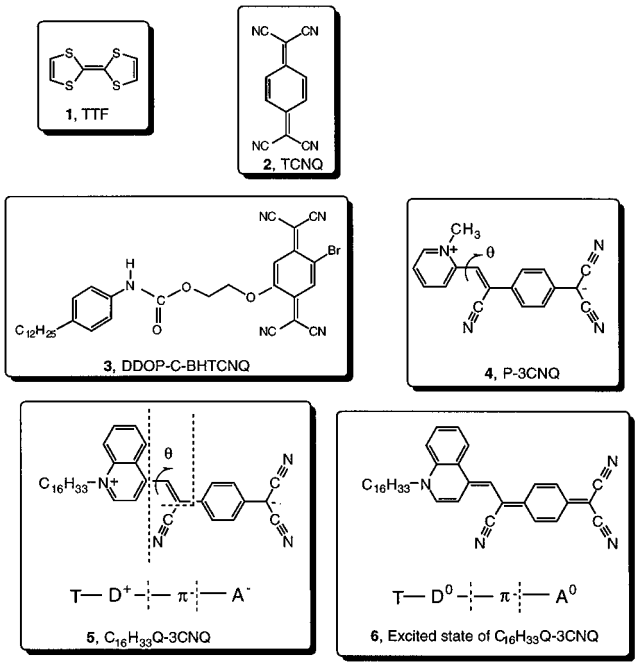

However, one such $D{-}\sigma{-}A$ molecule, namely DDOP−C−BHTCNQ, **3** (where D = DDOP = dodecyloxyphenyl = weak one-electron donor, C = carbamate = covalent σ bridge, A = BHTCNQ = bromo(hydroxyethoxy)tetracyanoquinodimethane = strong one-electron acceptor) showed electrical asymmetries in sandwiches

$$\text{Pt|LB multilayer of } \mathbf{3}\text{|Mg|Ag} \quad (3)$$

despite the fact that DDOP is a weak donor.[21]

A Schottky barrier could easily form[22] between Mg and TCNQ (the salt $Mg^{2+}(TCNQ^-)_2$ is known, and $Mg^{2+}TCNQ^{2-}$ can also form); therefore, the molecular origin of asymmetries seen in the measured currents of **3** was put into doubt.[22]

A new family of zwitterionic molecules was discovered by Ashwell and co-workers, a quaternary picolinium or lepidinium halide, when reacted with an alkali salt of TCNQ, can yield a class of ground-state zwitterions, whose first example is picolyltricyanoquinodimethane or picolinium tricyanoquinodimethanide (P-3CNQ, **4**), whose crystal structure[23] revealed that **4** is indeed a zwitterion, with a $\theta = 30°$ twist[23] between the pyridinium ring and the central six-membered ring of $3CNQ^-$, and a ground-state calculated dipole moment of 26 D (INDO; atom coordinates from the crystal structure).[23] These molecules, when made suitably amphiphilic by addition of a long alkyl terminations, yield Z-type Langmuir−Blodgett films that are excellent $\chi^{(2)}$ materials.[24] This class of molecules has a very narrow and solvatochromic absorption band.[24]

The most interesting member of this class is (*Z*)-β-*N*-hexadecyl-4-quinolinium-α-cyano-4-styryldicyanomethanide or γ-(*n*-hexadecyl)quinolinium tricyanoquinodimethanide, $C_{16}H_{33}Q$-3CNQ (**5**), which is blue in acetonitrile solution.[24] The

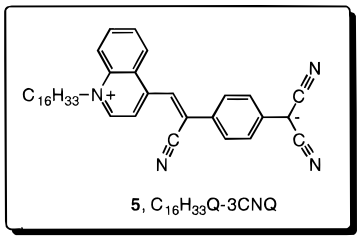

zwitterionic nature of **5** can be seen by calling it a $T{-}D^+{-}\pi{-}A^-$ molecule, where T is the hexadecyl "tail" (needed to help form good LB films), D^+ is the quinolinium moiety, π is the π-electron bridge, and A^- is the tricyanoquinodimethanide ($3CNQ^-$) moiety. **5** forms Z-type Langmuir−Blodgett (LB) multilayers with a very high $\chi^{(2)}_{zzz} = 180$ pm V^{-1}.[25] The blue narrow absorption band in solution may be due to an intervalence transfer band (IVT); when several molecules are packed in a multilayer, an additional intermolecular charge transfer band (ICT) may also occur. For a single crystal of **4**, these two bands had been identified securely by polarized spectroscopy.[26] It is believed[24−26] that the ground state of **5** is very polar, while its first excited state is less polar, of the type $T{-}D{-}\pi{-}A$ (**6**) and that the efficiency for frequency doubling is due to the transition

$$T{-}D^+{-}\pi{-}A^- \rightarrow T{-}D{-}\pi{-}A \quad (4)$$

In **5**, the quinolinium and tricyanoquinodimethanide rings may be twisted by some unknown angle θ (which was 30° for **4**[23]). The neutral excited state $T{-}D{-}\pi{-}A$ might be planar ($\theta = 0°$); if $\theta = 90°$ then IVT = 0, and the blue color should disappear.

When LB multilayers of **5** were sandwiched between a noble metal electrode (Pt or Ag) and a magnesium electrode (protected by an overlayer of Ag), then asymmetric currents through the laterally macroscopic multilayer indicated electrical rectification through the molecule[27]

$$\text{Pt|LB multilayer of } \mathbf{5}\text{|Mg|Ag} \quad (5)$$

and even in the sandwich:

$$\text{Pt|LB monolayer of } \mathbf{5}\text{|Mg|Ag} \quad (6)$$

(18) Metzger, R. M.; Panetta, C. A. *New J. Chem.* **1991**, *15*, 209−221.
(19) Metzger, R. M. In *Molecular and Biomolecular Electronics*; Birge, R. R., Ed.; ACS Advances in Chemistry Series 240; American Chemical Society: Washington, DC, 1994; pp 81−129.
(20) Metzger, R. M. *Mater. Sci. Eng.* **1995**, *C3*, 277−285.
(21) Geddes, N. J.; Sambles, J. R.; Jarvis, D. J.; Parker, W. G.; Sandman, D. J. *Appl. Phys. Lett.* **1990**, *56*, 1916−1918.
(22) Geddes, N. J.; Sambles, J. R.; Jarvis, D. J.; Parker, W. G.; Sandman, D. J. *J. Appl. Phys.* **1992**, *71*, 756−768.
(23) Metzger, R. M.; Heimer, N. E.; Ashwell, G. J. *Mol. Cryst. Liq. Cryst.* **1984**, *107*, 133−149.
(24) Ashwell, G. J.; Szablewski, M.; Kuczynski, A. P. In *Lower-Dimensional Systems and Molecular Electronics*; Metzger, R. M., Day, P., Papavassiliou, G. C., Eds.; NATO ASI Series; Plenum: New York, 1991; Vol. *B248*, p 647.
(25) Ashwell, G. J. In *Organic Materials for Nonlinear Optics*; Ashwell, G. J., Bloor, D., Eds.; Royal Soc. of Chem.: Cambridge, 1993; pp 31−39.
(26) Akhtar, S.; Tanaka, J.; Metzger, R. M.; Ashwell, G. J. *Mol. Cryst. Liq. Cryst.* **1986**, *139*, 353−364.
(27) Ashwell, G. J.; Sambles, J. R.; Martin, A. S.; Parker, W. G.; Szablewski, M. *J. Chem. Soc., Chem. Commun.* **1990**, 1374−1376.

Doubts raised about the Schottky barrier role of the Mg electrode[22] prompted the insertion of an insulating monolayer of a fatty acid between the metal electrodes and 3 monolayers of $C_{16}H_{33}Q$-3CNQ;[28] I−V asymmetries were still seen and ascribed to molecular rectification.[28]

The electrical rectification seen[28] for **5**, regardless of mechanism, has generated theoretical attention.[29,30] One important issue is whether the ground state is "zwitterionic", as shown in **5**, or "neutral", as shown in **6**. The theoretical studies[29,30] suggested that in the ground state a mixture of neutral and zwitterionic resonance forms may co-exist[30] and allow for intramolecular electron transfer in a monolayer in an adiabatic regime in the sense of Marcus−Hush theory.[31,32]

$$k_{ET} = \nu_a\{\pi^2\Delta^2[2h(\pi RT\lambda)^{1/2}]^{-1}\} \exp(-\Delta G^*/RT). \quad (7)$$

Here k_{ET} is the rate of electron transfer; ν_a is the frequency of formation of the activated complex, whose free energy of activation is ΔG^*; λ is the total Franck−Condon reorganization energy, i.e. the energy difference between the molecule before electron transfer (with its solvent atmosphere) and the molecule after the electron transfer (with its modified solvent atmosphere); Δ is the electronic coupling energy between the vibrational energy envelopes of the reactant and of the product at the point of their avoided crossing; h is Planck's constant; R is the gas constant; and T is the absolute temperature. The factor in { } is for "non-adiabatic" electron transfer; it becomes unity for an "adiabatic" transfer.

For a single molecule (monolayer) of **5**, Δ is large and rectification is explicable,[30] while for a multilayer, Δ is very small and rectification may be due to defect conduction.[30] Of course, if the twist angle θ in **5** becomes 90°, then the molecule must become a zwitterion.[30] It was suggested that **4** and **5** belong to a class of twisted internal charge transfer (TICT) systems.[30] However, such twisting would make the electron transfer process quite slow. The energy-minimized "gas-phase" theoretical calculations give for **4** a smaller ground-state dipole moment[29] than calculated for the geometry of **4** in the crystal,[23] unless efforts are made to account approximately for "solvent effects".[30] Theory suggested that in the first excited state $\theta \approx 90°$,[30] while for the ground state ("gas phase") $\theta = 9°-11°$.[30]

After two earlier preliminary studies of **5**,[33,34] we report here a novel, very convenient and efficient synthesis of **5**, confirm its ground-state zwitterionic structure, confirm electrical rectification by both LB monolayers and multilayers by macroscopic and nanoscopic methods, and identify incontrovertibly the direction of higher conductivity relative to the orientation of the molecules in the multilayers. We assert that **5** is a unimolecular rectifier.

2. Experimental Methods

NMR spectra were measured using Bruker 360 or 500 MHz spectrometers. UV spectra were measured on a Perkin-Elmer Sigma 3 spectrophotometer. Cyclic voltammograms were measured on a PAR 270 potentiostat, using a 10^{-4} M solution of **5** in CH_2Cl_2, a Pt wire working electrode, an SCE reference electrode, 0.1 M NBu_4ClO_4 electrolyte, and a scan rate of 20 mV/s.

To obtain the dipole moment of **5**, the dielectric constants of dilute solutions of **5** in dichloromethane were measured, as a function of temperature, at 1 kHz, using a coaxial capacitance cell (three concentric Pt cylinders, thickness 0.5 mm each, length 2.5 mm, diameters 8 (ground), 6, and 2 mm), a Hewlett-Packard 4263B LCR meter, and a Cole−Palmer refrigerated temperature bath. Because **5** is insoluble in nonpolar solvents, we used dichloromethane (gas-phase dipole moment $\mu = 1.60$ D[35]) and low solute concentrations ($<7.5 \times 10^{-2}$ mg/mL); results with acetonitrile ($\mu = 3.92$ D[36]) were irreproducible or physically meaningless. From the Kirkwood−Fröhlich equation,[37] an effective dipole moment, $g^{1/2}\mu$, can be extracted from temperature-dependent measurements:

$$g\mu^2 = [9kT(\epsilon - n^2)(2\epsilon + n^2)]/[4\pi N\epsilon(n^2 + 2)^2] = (9kT\Sigma)/4\pi N) \quad (8)$$

In eq 8, ϵ = dielectric constant, n = refractive index, T = absolute temperature, k = Boltzmann constant, N = number of molecules of **5** per unit volume, Σ = Onsager function $(\epsilon - n^2)(2\epsilon + n^2)/\epsilon(n^2 + 2)^2$, and g = Kirkwood correlation factor, discussed below. For n we used the refractive index of the pure solvent ($n = 1.42$). Measurements were done in the range −10 to 30 °C. For pure dichloromethane, we found $\mu = 1.67 \pm 0.83$ D.

Considering the molar polarization $P = 4\pi N_A\mu^2/9kT = \Sigma M/d$, where M is the molar mass, N_A is Avogadro's number, and d is the density, another approach for calculating the dipole moment of the solute[38] is to assume that the molar polarization of the solution P_{12} is given by

$$P_{12} = x_1P_1 + x_2P_2 \quad (9)$$

where x is the mole fraction and the subscripts 1 = solvent and 2 = solute.

Theoretical calculations were performed using the CAChe program package on a Macintosh PowerPC 8100AV microcomputer.

Pockels−Langmuir and Langmuir−Blodgett films were studied using both an analog Lauda film balance and also a microcomputer-controlled Nima Model 622D2 trough, both connected to a Lauda constant-temperature bath (5−30 °C), in a room with HEPA-filtered air, and "conductivity" water (Millipore Milli-Q, 18 MΩ cm). The Volta (Kelvin) electrostatic potential difference at the air−film interface was measured using a Monroe "Isoprobe" Model 162 electrostatic voltmeter, interfaced to the NIMA microcomputer; a monolayer of arachidic acid had $\Delta V = 0.31$ V. Substrates used were HOPG (Union Carbide Grade ZYA) or a single-crystal Au(111) (Goodfellow) and Al evaporated on glass.

Ellipsometric measurements were performed on a Rudolph Auto-EL-III ellipsometer ($\lambda = 632.8$ nm). X-ray diffraction measurements were performed using a Rigaku DX-1B powder diffractometer and Cu Kα X-radiation. Fourier transform infrared (FTIR) spectra were obtained on a Bruker IFS-88 spectrometer, using a grazing-angle accessory (Specac; angle of incidence 85°) and a wire polarizer (Specac). Scanning tunneling micrographs were obtained on Digital Instruments Nanoscope II and Nanoscope IIIa scanned probe microscopes, using a Pt/Ir tip and the type A head, the scanning tunneling spectroscopy (STS) software, and the CITS software.

An Edwards EL306A evaporator, with a multiple-source rotating stage, a liquid nitrogen-cooled cold finger, and a quartz film thickness monitor, was used to make both the base electrode (Al on quartz) and also the Al and/or Mg pads placed on top of the Langmuir−Blodgett monolayers and multilayers. The base pressure was 10^{-6} Torr; the distance from the evaporating source to substrate was 21 cm. After deposition of the LB film atop the Al base electrode, the substrate was dried at least 72 h in a desiccator in the presence of P_2O_5. Al, Mg, or Ag was evaporated on top of the LB film. The electrodes placed on

(28) Martin, A. S.; Sambles, J. R.; Ashwell, G. J. *Phys. Rev. Lett.* **1993**, *70*, 218−221.
(29) Broo, A.; Zerner, M. C. *Chem. Phys.* **1996**, *196*, 407−422.
(30) Broo, A.; Zerner, M. C. *Chem. Phys.* **1996**, *196*, 423−426.
(31) Marcus, R. A. *J. Chem. Phys.* **1965**, *43*, 679−701.
(32) Hush, N. S. *Trans. Faraday Soc.* **1961**, *57*, 557−580.
(33) Wu, X.-L.; Shamsuzzoha, M.; Metzger, R. M.; Ashwell, G. J. *Synth. Met.* **1993**, *55*−57, 3836−3841.
(34) Metzger, R. M.; Tachibana, H.; Wu, X.; Hopfner, U.; Chen, B.; Lakshmikantham, M. V.; Cava, M. P. *Synth. Met.* **1997**, *85*, 1359−1360.
(35) Weast, R. C., Ed. *Handbook of Chemistry and Physics*, 70th ed.; CRC Press: Boca Raton, FL, 1989; pp E-59−61.
(36) Ghosh, S. N.; Trambarulo, R.; Gordy, W. *J. Chem. Phys.* **1953**, *21*, 308−310.
(37) Böttcher, C. J. F.; Van Belle, O. C.; Bordewijk, P.; Rip, A. *Theory of Electric Polarization*; Elsevier: Amsterdam, 1973; Vol. 1, pp 245−284.
(38) Davies, M. *Some Electrical and Optical Aspects of Molecular Behaviour*; Pergamon: Oxford, 1965.

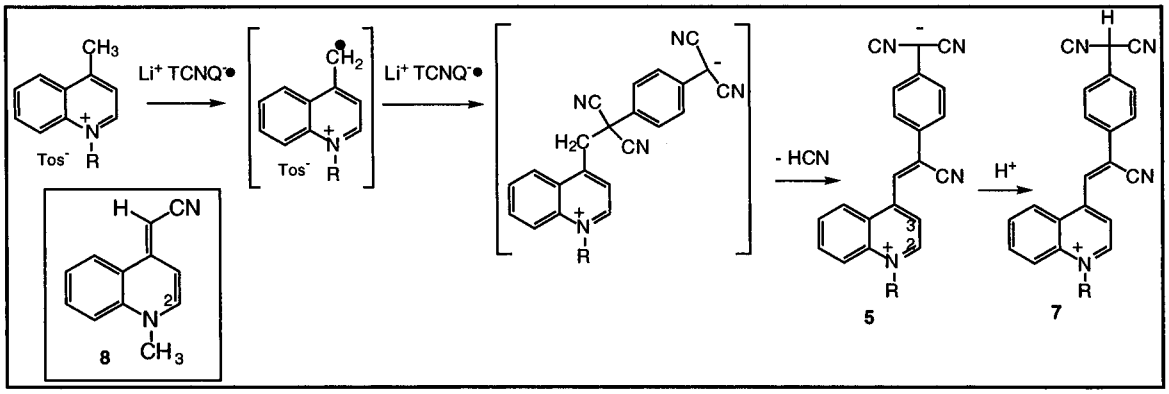

both the Al base and the Al pads were Au wires (diameter 0.05 mm) wetted either by a Ga/In eutectic or by Ag paste (GC Controls; better contacts were obtained by heating this paste to evaporate the butyl acetate solvent and redissolving it in *p*-xylene).

The current−voltage profiles were obtained both in the PAR 270 potentiostat (shorting the reference electrode to the counter electrode) and also in a Gateway 2000 microcomputer-controlled AC and DC conductivity measuring system, using a Hewlett-Packard Model 3245A universal source and an Hewlett−Packard Model 3457A multimeter.

3. Synthesis, NMR Spectrum, and Solution Visible−UV Spectra

Several syntheses of **5** have appeared in the literature,[39−41] all of which are erratic and tend to be unreliable as far as reproducibility. We now report a reproducible synthesis of **5**, starting from *N*-cetyllepidinium tosylate and the lithium salt of TCNQ radical anion, in dry DMSO solution in the presence of pyridine. We believe that this transformation occurs via an electron-transfer process. The lepidinium salt loses H$^{\bullet}$ to the $Li^+TCNQ^{\bullet-}$, being converted to a radical cation salt, which then couples with free $Li^+TCNQ^{\bullet-}$, to give an intermediate; spontaneous loss of HCN leads to the product.

The NMR spectrum of the compound is very diagnostic and corroborates previously cited IR and UV data indicative of a dipolar ground state.[40] The H-2 proton in **5** resonates at δ 9.39 ppm, giving a doublet with coupling constant J_{H-2H-3} of 5.80 Hz in DMSO-d_6 solution. Upon protonation to **7**, there is very little change in the H-2 resonance, which occurs at δ 9.23 (J_{H-2H-3} = 5.97 Hz), and a new singlet signal appears at δ 5.23 for the benzylic proton between the two cyano groups. The H-2 resonances are analogous to the α protons in a quinolinum salt. Furthermore, the H-2 proton in a 4-cyanovinyl *N*-alkylquinoline methide **8** resonates at δ 7.90 ppm.[42] The visible−ultraviolet spectrum of **5** is solvent-dependent, particularly the long-wavelength maximum in the visible region. In particular, this maximum is at 720 nm in CH_3CN, at 884 nm in CH_2Cl_2, and at 838 nm in $CHCl_3$. For the first two solvents the absorbance is linear with concentration, while in $CHCl_3$, there is a deviation (see Figure 1), presumably due to some intermolecular association at the higher concentrations (incipient admicelle or micelle formation?).

Synthetic Details. To a solution of *N*-cetyllepidinium tosylate (0.54 g, 1.00 mmol) and pyridine (0.27 g, 3.41 mmol) in dry DMSO (4 mL) was added $Li^+TCNQ^{\bullet-}$ (0.42 g, 1.99 mmol). This was heated on a steam bath for 1 h and cooled, and the blue crystalline solid (0.15 g, 28%) was filtered off. The mother liquor was heated further on the steam bath for 20 h and cooled, and the blue crystalline solid (0.17 g, 31%) filtered off. Total yield of product: 0.32 g, 59%. Recrystallization from pyridine furnished pure **5** as blue microcrystals: mp > 290 °C; UV−vis (DMSO) broad peak at λ_{max} = 687 nm; ^{1}H-NMR (DMSO-d_6) (330 K) δ 9.39 (d, 1H, J = 5.80 Hz), 8.74 (d, 1H, J = 8.50 Hz), 8.52 (d, 1H, J = 8.96 Hz), 8.45 (d, 1H, J = 6.35 Hz), 8.36 (s, 1H), 8.24 (t, 1H, J = 7.86 Hz), 8.01 (t, 1H, J = 7.72 Hz), 7.72 (d, 2H, J = 8.27 Hz), 6.90 (d, 2H, J = 8.59 Hz), 4.96 (t, 2H, J = 7.16 Hz), 2.00 (t, 2H, J = 7.40 Hz), 1.41−1.23 (m, 26H), 0.85 (t, 3H, J = 6.76 Hz); ^{13}C-NMR (DMSO-d_6) (330 K) δ 150, 147.34, 137.36, 134.84, 133, 129.21, 127.69, 127, 126.79, 122.90, 122.59, 121.34, 118.85, 118.18, 56.73, 30.91, 29.02, 28.63, 28.58, 28.48, 28.40, 28.27, 28.08, 25.50, 21.66; ^{1}H-NMR ($CDCl_3$/TFA) (protonated form **7**) δ 9.23 (d, 1H, J = 5.97 Hz), 8.45 (s, 1H), 8.37 (m, 2H), 8.30 (m, 2H), 8.07 (t, 1H, J = 6.31 Hz), 8.01 (d, 2H, J = 8.11Hz), 7.74 (d, 2H, J = 8.06 Hz), 5.23 (s, 1H), 5.0 (t, 2H, J = 5.45 Hz), 2.15 (m, 2H), 1.26 (m, 26H), 0.88 (t, 3H, J = 6.70 Hz). Anal. Calcd for $C_{37}H_{44}N_4$: C, 81.58; H, 8.14; N, 10.28. Found: C, 81.32; H, 8.19; N, 10.26. The blue microcrystals gave a superposition of diffraction patterns from several crystallites, which could not be resolved to provide an indexable diffractogram.

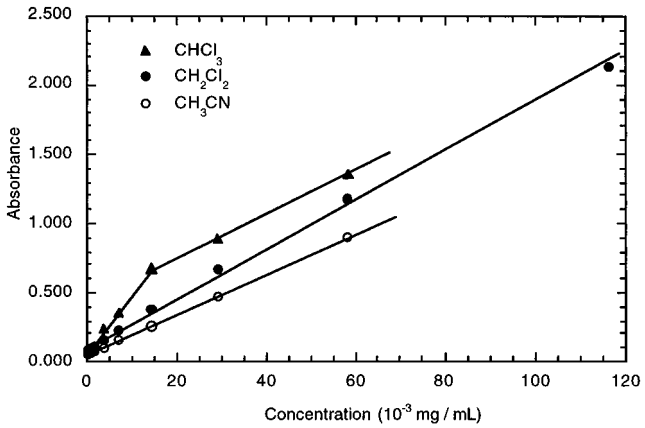

Figure 1. Absorbance vs concentration plot for a solution of **5** in CH_3CN (λ_{max} = 720 nm), in CH_2Cl_2 (λ_{max} = 884 nm), and in $CHCl_3$ (λ_{max} = 838 nm).

4. Cyclic Voltammogram

A cyclic voltammogram has been measured for **5**, and is shown in Figure 2. There is a one-electron quasi-reversible reduction ($E_{p,r}$ = −0.545 V, $E_{p,o}$ = −0.480 V, $E_{1/2}$ = −0.513 V vs SCE, ΔE = 0.065 V), a second irreversible reduction at

(39) Ashwell, G. J. *Thin Solid Films* **1990**, *186*, 155−165.
(40) Ashwell, G. J.; Dawney, E. J. C.; Kuczynski, A. P.; Szablewski, M.; Sandy, I. M.; Bryce, M. R.; Grainger, A. M.; Hasan, M. *J. Chem. Soc., Faraday Trans.* **1990**, *86*, 1117−1121.
(41) Ashwell, G. J.; Jefferies, G.; Dawnay, E. J. C.; Kuczynski, A.; Lynch, D. E. J.; Gongda, Y.; Bucknall, D. G. *J. Mater. Chem.* **1995**, *5*, 975−980.
(42) Hughes, T. V. Unpublished observation.
(43) Warren. B. L. *X-Ray Diffraction*; Addison-Wesley: Reading, MA, 1969; p 251.

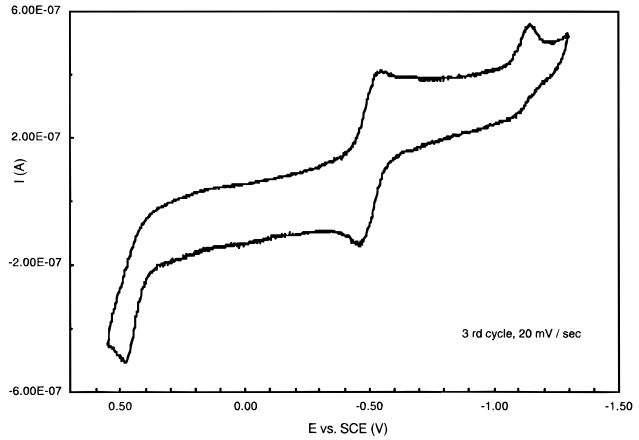

Figure 2. Cyclic voltammogram of a 10^{-4} M solution of **5** in CH_2Cl_2, measured using a Pt wire working electrode, an SCE reference electrode, 0.1 M NBu_4ClO_4 electrolyte, N_2 gas bubbled through the solution, and a scan rate of 20 mV/s.

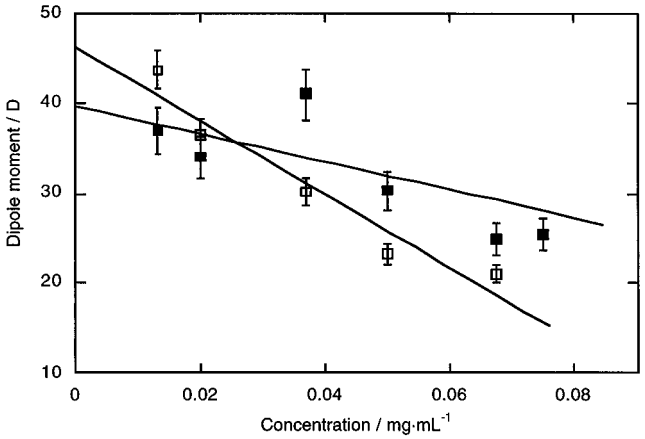

Figure 3. Effective dipole moments $g^{1/2}\mu$ of compound **5** in dichloromethane versus concentration, using the Kirkwood-Fröhlich equation, eq 8. (□) Data obtained directly from the temperature dependence of the dielectric constant of the solution (compound **5** + dichloromethane); at zero concentration the Kirkwood correlation factor should become $g = 1$. (■) Data obtained by "subtracting" the contribution of the slightly polar solvent, using eq 9. The solid lines are least-squares fits to the data.

$E_{p,r} = -1.16$ V, and an irreversible oxidation at $E_{p,o} = 0.49$ V vs SCE. Impurities in very small concentrations show an oxidation at 0.44 V and reductions at $E_{p,r} = -0.675$ V and $E_{p,r} = 0.383$ V vs SCE. Under identical conditions a solution of TCNQ, **2**, has a first reduction at $E_{1/2} = +0.214$ V vs SCE ($TCNQ^0 \rightarrow TCNQ^-$) and a second reduction at $E_{1/2} = -0.384$ V vs SCE ($TCNQ^- \rightarrow TCNQ^{2-}$); a sample of hexadecyl lepidinium bromide shows a reversible oxidation at $E_{1/2} = +0.70$ V vs SCE.

5. Dipole Moment

The effective dipole moments for various concentrations of **5** were calculated, using eq 8, from the slope of Σ versus $1/T$, and also from the partial molar polarization of the solute in the same temperature range. Figure 3 shows that equivalent results were obtained from both methods. The Kirkwood correlation factor g takes into account all intermolecular interactions, which lead to some mutual orientation of the molecular dipoles; a simple expression[37] is $g = 1 + z\langle\cos\theta_{ij}\rangle$, where z is the average number of neighboring molecules around a given dipole and $\langle\cos\theta_{ij}\rangle$ is the average of the cosine of the angle between two dipoles; for infinitely dilute solutions, g tends to 1.[37] Thus, the extrapolation of the results to zero concentration (Figure 3) yields a dipole moment of 40−45 D (let us say 43 ± 8 D) for **5** in dichloromethane at infinite dilution.

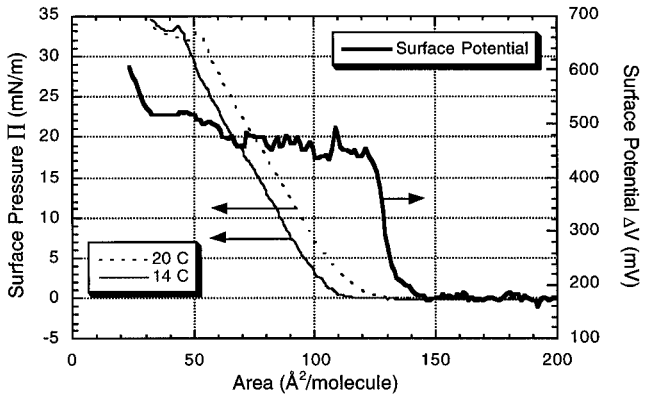

Figure 4. Pressure−area isotherms for **5** at 14 and 20 °C and surface (Volta or Kelvin probe) potentials at 14 °C.

This result strongly supports the zwitterionic nature of the ground state of **5**, as also established by NMR (see section 3). Theoretical calculations have determined the ground-state dipole moments of **4** (crystal geometry) to be $\mu = 26.16$ D;[23] for **4** and **5**, "gas-phase" calculations yield $\mu = 8-11$ D;[29] for **5**, including "solvent effects", $\mu = 29.6$ D.[30] A factor of ca. 1.5 between theory and the present experiments seems reasonable, considering the inherent inaccuracy of theoretical methods, and the approximations used in analyzing the experimental data. Interactions between **5** and the solvent molecules can increase the real gas-phase dipole moment of **5**. The decrease of the effective dipole moment, when increasing the concentration, indicates that molecules of **5** tend to align with anti-parallel dipoles ($g < 1$).

6. Pockels−Langmuir Monolayers at the Air−Water Interface

The pressure−area (Π−A) isotherm of **5**, when measured in sunlight or under fluorescent light, shows a collapse area $A_c = 34 \pm 1$ Å^2 molecule^{-1} at the collapse pressure $\Pi_c = 43.5$ mN m^{-1} and a limiting area $A_o = 125 \pm 1$ Å^2 molecule^{-1} at zero film pressure [39], but with additional intermediate monolayer ordering transitions at $\Pi = 27$ mN m^{-1} ($A = 58$ Å^2 molecule^{-1}) and $\Pi = 30$ mN m^{-1} ($A = 43$ Å^2 molecule^{-1}), where the molecules are inclined to the water surface.[39,44]

The Π−A isotherm of **5**, when measured under a green safelight, shows very clearly a collapse point at 50 Å^2 molecule^{-1} and 34 mN m^{-1} (Figure 4): this isotherm is moderately temperature-dependent; the collapse point at 50 Å^2 molecule^{-1} and 34 mN m^{-1} was not noticed in the first report.[39] The Volta potential difference ΔV is set to zero before spreading the monolayer, rises to about 0.18 V at the start of the compression, and becomes about $\Delta V = 0.46$ V at about 120 Å^2/molecule, i.e. before the monolayer is fully compressed: the dipolar layer is more polar than, e.g., cadmium arachidate.

7. Langmuir−Blodgett Films: X-ray and UV−Visible Spectra of Multilayers

The LB transfer of monolayers and multilayers of **5** was performed at 15 mm min^{-1} using a film pressure of 20 mN m^{-1}. Molecule **5** first transfers on the downstroke onto hydrophobic HOPG and on the upstroke onto a freshly cleaned hydrophilic Au(111) single crystal and on an Al electrode. The hydrophobic hexadecyl "tail" of D^+ is thought to be the end of

(44) Wu, X. Ph.D. Dissertation, University of Alabama, 1995.

the molecule closest to HOPG, while the hydrophilic 3CNQ$^-$ (A^-) end should be closest to Au(111). At the lower transfer speed of 15 mm min^{-1} the LB multilayers (past the first monolayer) are Z-type, while at the faster transfer speed of 45 mm min^{-1}, the LB multilayers become Y-type.

X-ray diffraction spectra, taken several days after film transfer onto a glass substrate, shows that the Y-type films apparently reorder to Z-type after transfer, with a thickness of 23 Å per monolayer and a longitudinal crystallite correlation length[43] of 200 Å ($2\theta = 3.81°$; Scherrer linewidth at half-height 0.4° in 2θ). Thus, for multilayers, the Z-type ordering is more stable.

LB multilayers of **5** transferred onto HOPG at 15 mm min^{-1} have orientation

$$\text{HOPG}|\rightarrow\leftarrow\leftarrow\leftarrow\leftarrow\leftarrow\leftarrow\leftarrow \text{ etc.} \qquad (10)$$

Here the arrow $\rightarrow$ indicates the rough molecular orientation; it points from the hexadecyl tail T and the quinolinium ring D^+ (tail of arrow) toward the dicyanomethylene head of A^- (head of arrow). As shown in eq 10, the first monolayer adheres with the hexadecyl tail T next to HOPG (X-type orientation), while the other layers (second through 15th) have Z-type orientation (tails away from HOPG). The transfer ratios were measured to be about 50% for the first layer, and from 50% to 100% for the Z-type layers.

The film transfer to Al is Z-type throughout

$$\text{Al}|\leftarrow\leftarrow\leftarrow\leftarrow\leftarrow\leftarrow\leftarrow \text{ etc.} \qquad (11)$$

but the transfer ratio for the first layer is now over 90%.

A sharp and narrow absorption band peaked at 570 nm is found for LB films transferred onto a quartz substrate at 14 °C in the dark and measured at 25 °C (Figure 5). This narrow band disappears if the films are protonated but returns when exposed to ammonia vapor;[41] it disappears irreversibly if the film, or the solution, is exposed to bright light and air for some time.

8. Theoretical Calculations

A geometry-optimized PM3 calculation was performed for **5** (heat of formation 6.02 eV). The molecule **5** is twisted; the angle between the quinolinium ring and the central phenyl ring of 3CNQ is ≈30°. The computed dipole moment for the ground state singlet of **5** is 10.7 D, with the highest occupied molecular orbital (HOMO) at −7.98 eV (MO #106, localized on quinolinium, the π bridge, and the 3CNQ end) and the lowest unoccupied molecular orbital (LUMO) at −2.42 eV (MO #107, localized on 3CNQ$^-$); however, the bond lengths in the molecule are more quinonoid than benzenoid. When using a shorter alkyl chain (octyl instead of hexadecyl) and AM1,[44] the ground state has dipole moment of 10.56 D and a heat of formation of 7.61 eV, while the excited singlet state has a smaller dipole moment, 6.36 D, and a heat of formation of 10.83 eV, i.e. 3.22 eV higher.[44] A recent PM3 calculation for the excited singlet state of **5** yielded a heat of formation of 8.469 eV, a twisted geometry ($\theta \approx 90°$), and a high dipole moment of 45.4 D. These results agree with ref 30. The inferred approximate molecular size for **5** is 33 Å × 7 Å × 4.5 Å.

9. Ellipsometry

The thickness per monolayer, measured by ellipsometry (λ = 670 nm) and by surface plasmon resonance, is 22 ± 2 Å;[41] thus the approximate molecular axis may be tilted 48 ± 5° from the normal to the monolayer plane. A larger apparent thickness (26 ± 2 Å, $n = 1.50 \pm 0.05$, $\kappa \equiv 0$), measured by ellipsometry (HeNe laser, λ = 632.8 nm), is less reliable because at 632.8 nm the molar absorptivity is not negligible (see Figure 4), so the assumption $\kappa = 0$ is not valid.

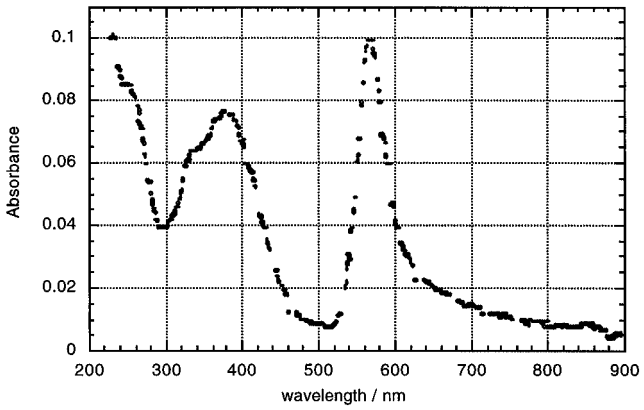

Figure 5. Visible spectrum of an 11-layer LB film of **5** transferred onto quartz; the narrow absorbance has a peak at 570 nm (2.17 eV; spectral width at half-maximum = 0.19 eV); the absorbance per monolayer at 633 nm is estimated as 0.0021.

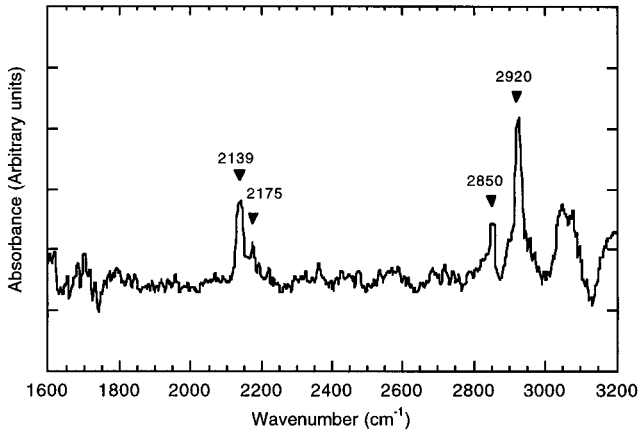

Figure 6. p-Polarized grazing-angle FTIR spectrum ($\theta = 85°$) of LB monolayer of **5** on Al.

10. Infrared Spectra

Grazing-angle Fourier transform infrared spectra, using p-polarized light for a monolayer of **5** on a glass substrate covered by Al (Figure 6), shows absorbances at 2850 cm^{-1} (symmetric C−H), 2920 cm^{-1} (asymmetric $-CH_2-$), 2139 cm^{-1} (−C≡N), and 2175 cm^{-1} (−C≡N), indicating that the cyano groups and the methylene groups do not lie in the plane of monolayer but are somewhat tilted from it. The CN stretches show evidence of shifts due to partial charge: negatively charged C≡N groups (2175 cm^{-1}) and a shifted C≡N group (2139 cm^{-1}). For a monolayer of **5** on either Au(111) or HOPG, the C−H and $-CH_2-$ signals can be seen clearly; a −C≡N signal at 2175 cm^{-1} is barely visible for the monolayer on Au(111).[44]

11. Macroscopic Conductivity of LB Films

An Edwards 306A evaporator and a PAR 270 potentiostat were used to study macroscopic "metal|organic|metal" sandwiches. The glass or quartz or silicon substrates were covered by 25 mm × 75 mm × 100 nm thick Al layer, then LB monolayer or multilayer films were transferred under a green safelight, then the sample was dried for 2 days in a vacuum desiccator containing P_2O_5. Twelve cylindrical "pads" of Al (four each of areas 2.8, 4.5, and 6.6 mm^2, all either 100 or 300 nm thick, depending on the run) were finally deposited per microscope slide, atop the organic layer, with the substrate

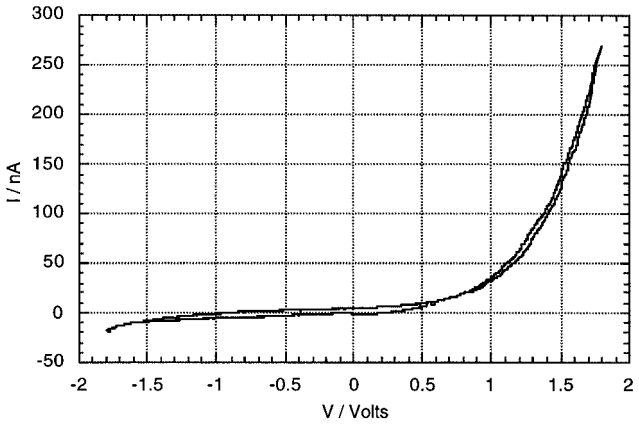

Figure 7. Conductivity of a sandwich "Ga/In eutectic|Al (100 nm)|4LB monolayers of **5** (Z-type)|Al (100 nm)|Ga/In eutectic". The scan rate was 100 mV/s. The counter and reference electrodes (shorted together) are connected to one Al electrode; the working electrode is connected to the other Al electrode. The direction of easier electron flow ($I > 0$ for $V > 0$) is from the bottom electrode through the film to the top electrode.

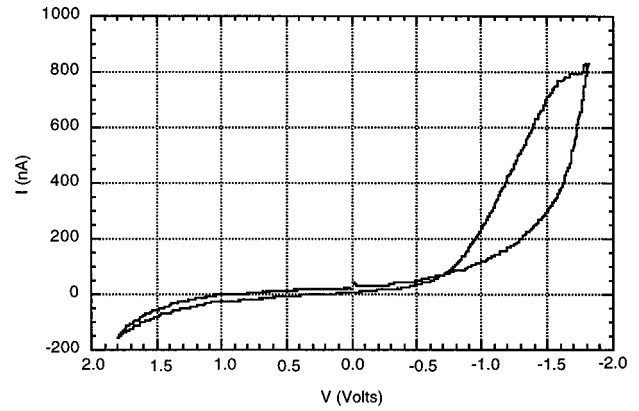

Figure 8. Conductivity of a sandwich "Ga/In eutectic|Al (100 nm)|4LB monolayers of **5** (Z-type)|Mg (110 nm)|Al (100 nm)|Ga/In eutectic". The counter and reference electrodes (shorted together) are connected to one Al electrode; the working electrode is connected to the other Al electrode. The direction of easier electron flow ($I > 0$ for $V > 0$) is from the bottom electrode through the film to the top electrode.

cooled to 77 K, to form the sandwich

$$\text{glass|Al|4 LB monolayers of } \mathbf{5}\text{|Al} \qquad (12)$$

as shown in Figure 7. Also, to duplicate the work of ref 28, Mg was coated atop the organic film (110 nm), and then the sample was covered by the top Al pad without breaking vacuum, thus achieving the sandwich

$$\text{glass|Al|4 LB monolayers of } \mathbf{5}\text{|Mg|Al} \qquad (13)$$

Contact to the Al electrodes was achieved using either a Ga/In eutectic, or Ag paste. Note that the electrodes (Al) are symmetrical in eq 12. Note also that, while drying multilayers of arachidic acid before depositing the top electrode was essential (spurious rectification is seen with wet multilayers), this problem is not serious for **5**: samples strongly dried in a vacuum desiccator with P_2O_5 showed essentially the same I−V characteristics as samples kept in the desiccator over $CaSO_4$ for a longer time. In all cases, reversing the electrode connections reversed the direction of rectification.

The work with multilayers gave equivalent results using the potentiostat or the I−V measurement setup. The work with monolayers was, predictably, much more difficult.

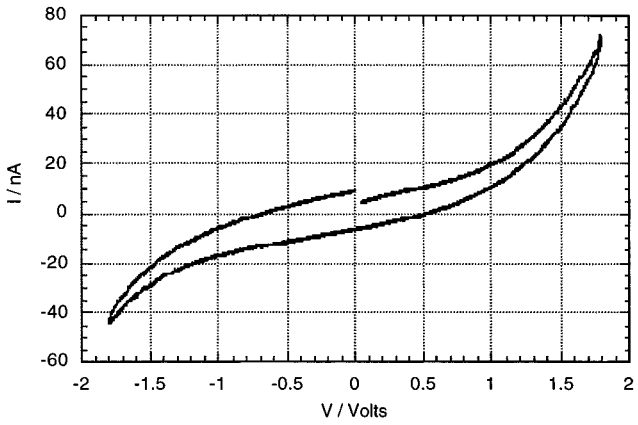

Figure 9. Conductivity of a sandwich "Ga/In eutectic|Al (75 nm)|1LB monolayer of **5** (Z-type)|Al (150 nm)|Ga/In eutectic". $V > 0$ means electron flow from the bottom electrode through the LB monolayer to the top electrode; the rectification ratio is low.

Of 39 "pads" checked (20 with areas of 2.8 mm^2, 15 with areas of 4.5 mm^2, 4 with areas of 6.6 mm^2) with two thicknesses of the Al pad (12 with thickness 300 nm, 27 with thickness 100 nm), 17 were electrical short circuits, either because of monolayer defects or because the Ga/In or Ag paste "made" defects. The 22 "good" junctions had DC resistances from 1 to 400 MΩ; of these, only four exhibited rectifying behavior. Figure 11a shows a typical rectification curve. Above a threshold voltage V_t, the monolayer shows higher currents for positive voltage than for the corresponding negative voltage. This V_t varies from junction to junction in the range $V_t = 0.8-1.3$ V.

The rectification ratio RR, defined by

$$\text{RR} = (\text{current at } V_o)/(\text{current at } -V_o) \qquad (14)$$

where V_o is the highest positive bias used, ranges from 2.4 to 26.4 the first time the film is measured. As the cycle is repeated, RR drops steadily and disappears after 4−6 cycles. Similarly, by applying a constant positive or negative bias, we observed a slow decrease, over 15−20 min, of the current for both polarities. It appears that, under the intense electric fields, the molecular dipoles reorient to minimize energy. For some of the junctions, short circuits form across the monolayer during the measurement.

In the range −0.5 to 0.5 V, the I−V characteristic is ohmic. In the reverse regime (negative bias), the logarithm of the current is linear with the applied bias (through-space tunneling) from −0.5 V to the highest negative bias applied (−1.5 V or −1.8 V). In the forward regime, we again observed $\ln_e(I) \propto V$ for $V > 0.5$, up to a threshold voltage (in the range 0.8−1.3 V, sample dependent), above which the current rises severalfold. This deviation from the $\ln_e(I) \propto V$ law may be ascribed to an enhanced through-bond electron transfer. This behavior resembles that observed by Martin et al. for multilayers of **5**.[28]

The results on both monolayers and multilayers show that the electrons preferentially flow by IVT from 3CNQ (A^-) to quinolinium (D^+), in agreement with the AR ansatz. In the case of multilayers, electron transfers between successive monolayers from the D^+ of layer N to the A^- of layer N-1 is possible (by tunneling through the alkyl chains), provided that the electric field is high enough to move the electron between the relevant molecular orbitals.

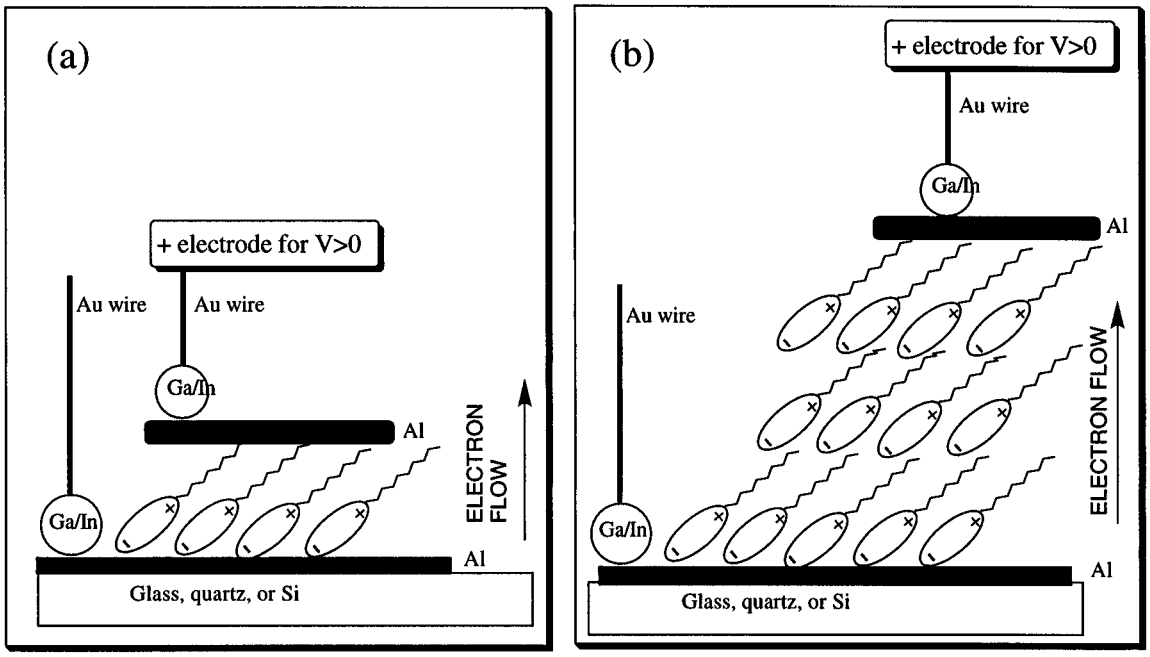

Figure 10. Orientation of the LB monolayer (a) or multilayer (b) on the glass, quartz, or Si substrate; the electrode (+) for positive bias, and the direction of "easy" electron flow for $V > 0$ are marked. In some cases Ag paste was used instead of the Ga/In eutectic.

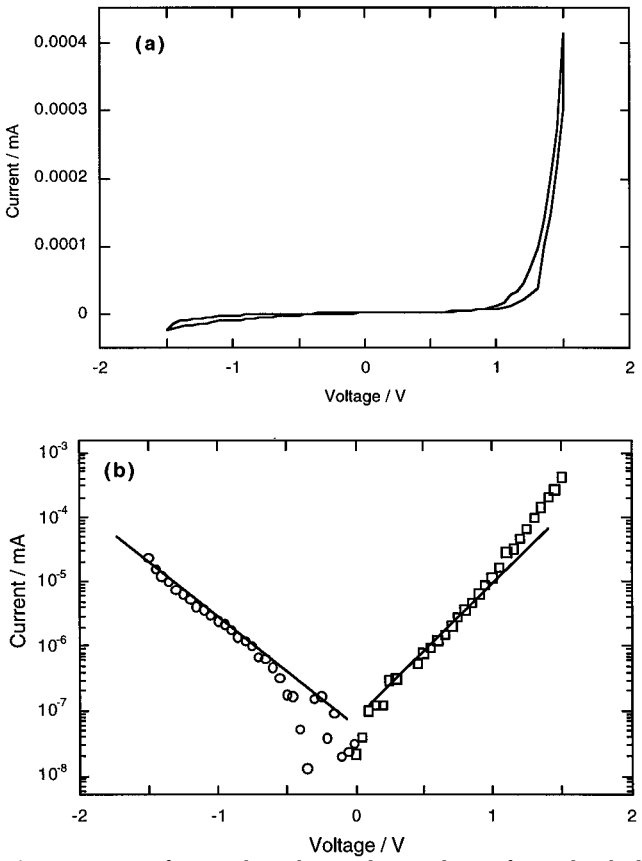

Figure 11. Rectification through a single monolayer of **5** sandwiched between Al electrodes (top Al pad area 4.5 mm^2, thickness 100 nm), using Ga/In eutectic and Au wires. The dc voltage is swept at a rate of 10 mV s^{-1}. (a) Linear plot of the DC current I versus the dc applied voltage *V*. (b) Plot of $\log_{10} I$ versus *V*.

12. Nanoscopic Structure of LB Films

With a modified Nanoscope II (preamplifier modified to allow for 100 times more current than usual) a Langmuir-Schaefer[45] monolayer of **5** deposited on HOPG an image with surprising resolution (Figure 12) was seen: this seemed to show the molecules, viewed with a Pt/Ir nanotip, seen from the dicyanomethylene end.[33] The repeat area of 4.5 × 13 Å consists of a "light" region (closer to the nanotip) of about 4.5 × 7 Å, plus by a dark region (4.5 × 6 Å). A solution drop of **5** in dimethyl sulfoxide also shows a repeat area of 4.5 × 13 Å.[33,44] Using a low-current STM (Nanoscope III) an LB monolayer of **5** showed a similar image, albeit at lower resolution, with repeat distance of 6 × 12 Å (Figure 13). As discussed below, these image are consistent with the molecules viewed end-on.

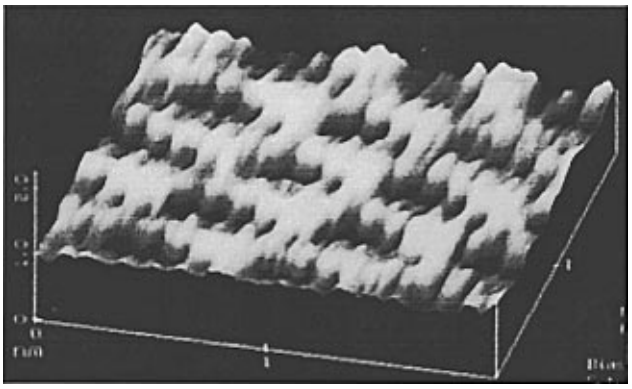

Figure 12. STM micrograph of Langmuir−Schaefer monolayer of **5** on HOPG, viewed with a Pt/Ir nanotip (Nanoscope II). Scan size = 2 nm × 2 nm, nominal setpoint currrent = 1.3 nA (actual = 130 nA), and bias = 92.5 mV. Adapted with permission from ref 33. Copyright 1993 Elsevier Science.

13. Nanoscopic Conductivity of LB Films

An earlier effort by scanning tunneling microscopy of LB monolayers of **5** on HOPG showed no reproducible asymmetries in the scanning tunneling spectroscopy (STS) I−V plots.[33]

Multilayers of **5** on HOPG were studied using a Pt/Ir nanotip at room temperature in air by STM and STS. Clear asymmetries

(45) Langmuir, I.; Schaefer, V. J. *J. Am. Chem. Soc.* **1938**, *60*, 1351−1360.

(46) Jin, C.; Haufler, R. E.; Hettich, R. L.; Basich, C. M.; Compton, R. N.; Puretzky, A. A.; Demyanenko, A. V.; Tuinman, A. A. *Science* **1994**, *263*, 68.

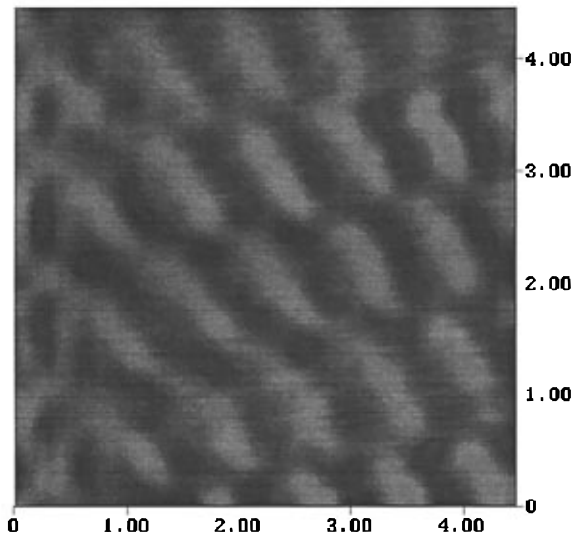

Figure 13. STM image of a LB monolayer of **5** on HOPG, with Pt/Ir tip (Nanoscope III). Scan size = 4.5 nm × 4.5 nm, *Z*-range = 2.3 pA, bias = −316 mV, and setpoint current = 3.2 pA.

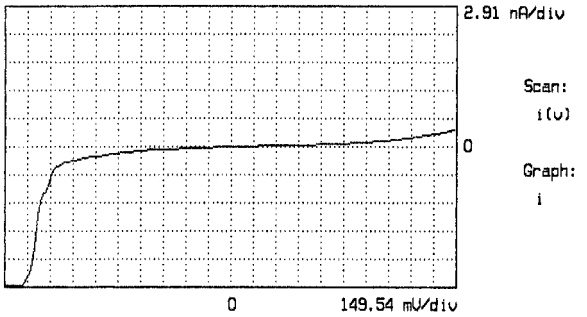

Figure 14. STS I−V curve for an LB film of 15 Z-type monolayers of **5** on HOPG, with Pt/Ir tip. The higher current for $V < -1.35$ V corresponds to electron flow from HOPG through molecules to the Pt tip.

in the I−V plot was seen in 15-layer films (Figure 14), but the corresponding STM images were of a graphite superstructure. In agreement with the I−V characteristics of multilayers sandwiched between Al electrodes, the STS current is consistent with electrons flowing by intramolecular intervalence electron transfer (IVT) between LB layers 2−15, and with "jumping over" layer 1 (Figure 15), but as discussed above, the electrons must somehow jump between adjacent monolayers. The current must somehow also jump over the first monolayer (which is directed the "wrong way" and is afflicted with a poor transfer ratio).

However, STM images (using a Pt/Ir nanotip, and setpoint currents of 1 nA) of a saturated solution of **5** dissolved in dimethyl sulfoxide (DMSO) on HOPG (not an LB film) show an asymmetric STS spectrum (Figure 16): higher currents are seen at negative bias (40 nA at −1.0 V) than at positive bias (<2 nA at +1.0 V). An STS spectrum for a monolayer of **5** shows a slightly higher current at positive bias, in the expected direction for the first (partial) monolayer on HOPG, adhering with the alkyl tail onto the HOPG surface (Figure 17).

14. Review of the AR Ansatz

Before discussing whether an AR mechanism, or a modification of it, is operative for $C_{16}H_{33}$Q-3CNQ, we should review the essentials of the AR ansatz.[17] The AR model of unimolecular rectification places a single molecule D−σ−A (D = good electron donor, A = good electron acceptor, σ = covalent linkage between D and A) between two macroscopic metal electrodes M_1 and M_2 with work functions ϕ_1 and ϕ_2, respectively. Under "forward bias" an electron is transferred from M_2 to M_1 in two steps:

$$M_1|D-\sigma-A|M_2 \xrightarrow{\text{step 1, ET}} M_1^-|D^+-\sigma-A^-|M_2^+ \quad (15)$$

$$M_1^-|D^+-\sigma-A^-|M_2^+ \xrightarrow{\text{step 2, IVT}} M_1^-|D-\sigma-A|M_2^+ \quad (16)$$

In eq 15 one electron hops (elastic tunneling, ET) from the HOMO of the neutral donor molecule, through a chemisorptive barrier, onto the Fermi level of the metal electrode M_1 whose ϕ_1 at the same energy as, i.e. in resonance with, the HOMO. Thus one electron is added to the metal conduction band, forming, formally, M_1^- and leaving the donor as the donor radical cation D^+. Similarly, an electron from the Fermi level of the metal electrode M_2 hops through a chemisorptive barrier onto the LUMO of the neutral acceptor molecule, which is at resonance with ϕ_2. This forms the acceptor radical anion A^- and removes one electron from the metal conduction band to form M_2^+. This leaves the molecule as an excited-state zwitterion $D^+-\sigma-A^-$.

In eq 16, an intervalence transfer (IVT) occurs: since the LUMO of the neutral acceptor A (A = TCNQ) is about 3 eV higher than the HOMO of the neutral donor D (D = TTF), therefore down-hill inelastic tunneling ensues through the molecule (through-bond tunneling), and the molecule returns to its ground state D−σ−A, but one electron has been moved by steps 1 and 2 from M_2 to M_1. It is guessed that the $D^+-\sigma-A^-$ state lies about 1−2 eV above the D−σ−A ground state.

Since good organic one-electron donors are terrible acceptors and good electron acceptors are terrible donors, therefore, the "reverse bias" process (step 3, eq 17; not shown in Figure 17) would involve an excited state that is estimated to be ≥4 eV higher than the excited state $D^+-\sigma-A^-$ and can be thus neglected.

$$M_1|D-\sigma-A|M_2 \overset{\text{step 3, ET}}{\not\rightarrow} M_1^+|D^--\sigma-A^+|M_2^- \quad (17)$$

(The only "hermaphroditic" donor that is an equally good acceptor is graphite, for which no rectification would occur).

Since step 3, eq 17, is unlikely, but steps 1 and 2, eqs 15 and 16, are favored, molecular rectification should occur. A competing "reverse-bias" process is autoionization (step 4, eq 18), followed by charge migration to the two metal electrodes (step 5, eq 19):

$$M_1|D-\sigma-A|M_2 \xrightarrow{\text{step 4}} M_1|D^+-\sigma-A^-|M_2 \quad (18)$$

$$M_1|D^+-\sigma-A^-|M_2 \xrightarrow{\text{step 5, IVT, ET}} M_1^+|D-\sigma-A|M_2^- \quad (19)$$

The AR process will work if step 1, eq 15, is much more likely than step 4, eq 18, and if the through-molecule tunneling in step 2, eq 16, is much larger than elastic through-space tunneling. The situation is reviewed diagrammatically in the top half of in Figure 18.

15. The Case of a Ground-State Zwitterion

The AR ansatz can be adapted (Figure 18, bottom six frames) to the ground-state zwitterion $D^+-\pi-A^-$, whose first excited

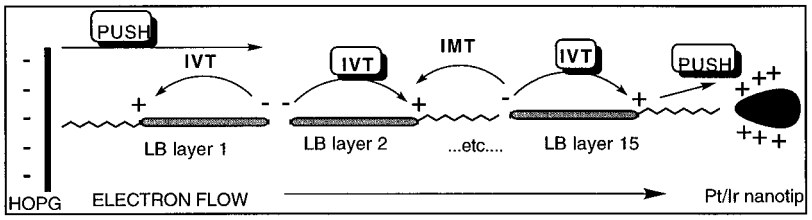

Figure 15. Direction of observed STS electron current through 15-layer LB multilayer of **5**.

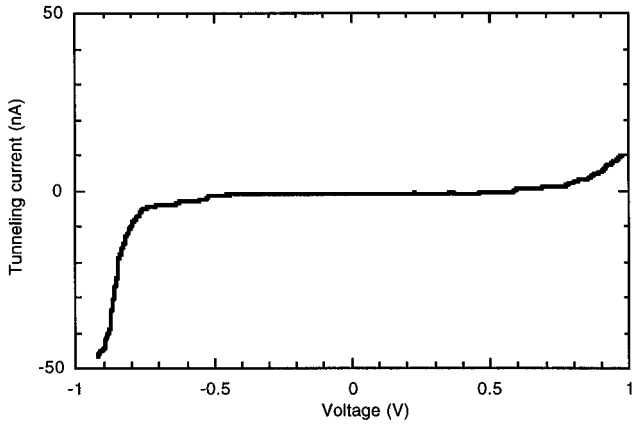

Figure 16. STS I−V curve for a DMSO solution drop of **5** on HOPG, with Pt/Ir tip (Nanoscope II). The higher current for $V < -1.35$ V corresponds to electron flow from HOPG through molecules to the Pt tip.[44]

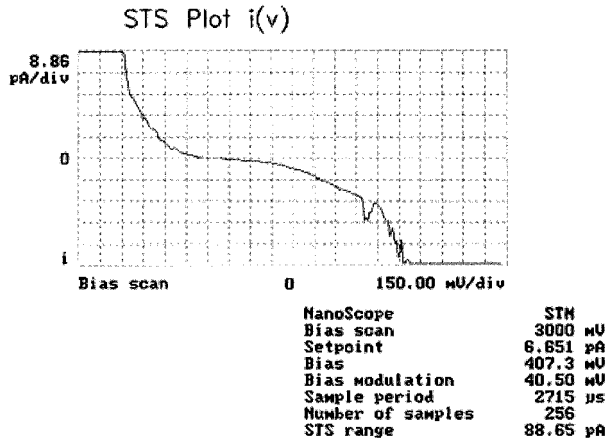

Figure 17. STS I−V curve for an LB monolayer of **5** on HOPG, with Pt/Ir tip (Nanoscope III). The higher current for $V > 0.5$ V corresponds to electron flow from Pt/Ir nanotip through molecules to HOPG.

state is the neutral molecule $D^0-\pi-A^0$. Under "forward bias" an electron is transferred from M_2 to M_1 in two steps

$$M_1|D^+-\pi-A^-|M_2 \xrightarrow{\text{step 6, IVT}} M_1|D^0-\pi-A^0|M_2 \quad (20)$$

$$M_1|D^0-\pi-A^0|M_2 \xrightarrow{\text{step 7, ET}} M_1^-|D^+-\pi-A^-|M_2^+ \quad (21)$$

The reverse bias process is

$$M_1|D^+-\pi-A^-|M_2 \xrightarrow{\text{step 8, ET}} M_1^+|D^0-\pi-A^0|M_2^- \quad (22)$$

$$M_1^+|D^0-\pi-A^0|M_2^- \xrightarrow{\text{step 9, IVT}} M_1^+|D^+-\pi-A^-|M_2^- \quad (23)$$

The system would rectify (steps 6 and 7, eqs 20 and 21), so that electrons are moved from M_2 to M_1, provided that step 8, eq 22, is less likely than step 6, eq 20.

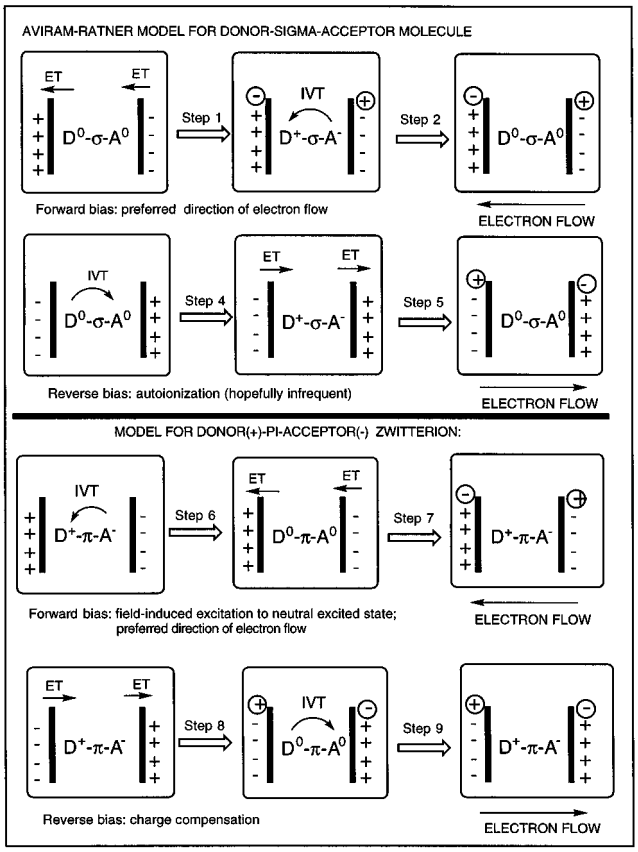

Figure 18. Depiction of electron transfers within D−σ−A molecules and $D^+-\pi-A^-$ zwitterions and to and from two metal electrodes, according to the AR model for neutral D−σ−A molecules (top six frames) and to the modified AR model for $D^+-\pi-A^-$ zwitterions (bottom six frames). Steps 1 and 2 are the preferred direction of electron flow (right to left) for D−σ−A, and steps 6 and 7 are the preferred direction of electron flow (right to left) for $D^+-\pi-A^-$ zwitterions.

16. Discussion

We have vastly improved on the synthesis of **5** by using a 2:1 molar ratio of TCNQ to quinolinium salt: this ensures the activation of the quinolinium ring needed for coupling. The ground state of the molecule is clearly zwitterionic, as demonstrated by its NMR spectrum and its measured solution dipole moment $\mu = 43 \pm 8$ D $= (1.4 \pm 0.3) \times 10^{-24}$ C m; this value corresponds to an electron−hole pair separated by 9 ± 1 Å, a large separation indeed: the estimated interatomic distance from the bridgehead C atom in the dicyanomethylene end of **5** to the quinolinium N atom is 10.5 Å. The monolayer thickness (23 Å by X-ray diffraction, 22 ± 2 Å by ellipsometry and surface plasmon resonance) suggest molecules inclined by 45−55° from the surface normal. The oxidation of **5** in dichloromethane solution is irreversible; its first reduction is reversible, but **5** is not a powerful electron acceptor. There is no electrochemical activity between 0.4 and −0.4 V vs SCE in CH_2Cl_2 solution.

The distance between the two N atoms of the dicyanomethylene end of **4**[23] is 4.385 Å; adding 2*N* van der Waals radii

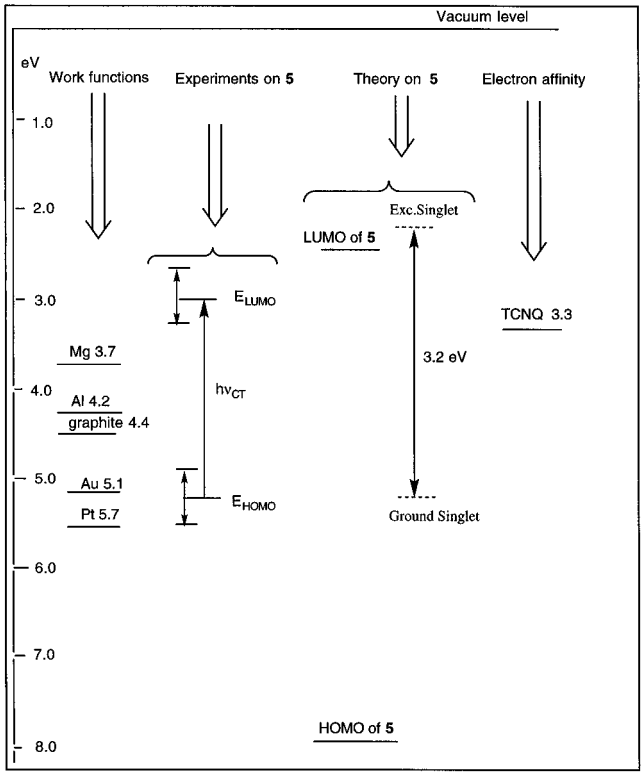

Figure 19. Approximate work functions of electrodes, electron affinity of TCNQ, and of HOMO and LUMO levels (experiment and theory) of molecule **5**, all relative to the vacuum level.

yields a calculated width of 7.4 Å for the dicyanomethylene end of **5**. Adding 5 Å for the part of the quinolinium ring not eclipsed by 3CNQ yields a total width of 12.4 Å, not far from the STM width of 13 Å (Figures 12 and 13). The van der Waals thickness of an aromatic ring (about 3.5 Å) must be increased by the presumed noncoplanarity of the quinolinium ring and the 3CNQ ring, so a thickness of about 4.5 Å is reasonable. Thus, STM repeat areas of 4.5 × 13 Å (Figure 12) or 6 × 12 Å (Figure 13) are roughly consistent with the calculated molecular cross-section and with the observed collapse area of 50 Å^2 at 20 °C (Figure 4).

The rectification by a monolayer of **5** on HOPG (Figure 17), with higher electron flow at positive bias from nanotip to HOPG, is seen often and is consistent with IVT across a molecule oriented with the dicyanomethylene end closer to the Pt/Ir nanotip (cf. LB layer 1 in Figure 15), but the monolayer adheres poorly to HOPG and is easily moved across the surface by the tip, so other, symmetric STS curves (through-space tunneling) are also seen.

The STS rectification across an LB multilayer (Figure 14) is very reproducible; the direction of higher electron flow at $V < -1.35$ V corresponds to IVT electron flow *within* layers 2−15 of a 15-layer film, as explained in Figure 15 (boxed IVT), but the contrary flow across layer 1 (IVT) and the electron flow mechanism between layers (IMT) are not explained.

The STS rectification by a solution drop (Figure 16) and its STM structure at the HOPG surface suggest that the molecules of **5** orient on the HOPG surface and show the same electrical behaviour as an LB multilayer of **5**. Monolayer rectification between Al electrodes (Figure 11) can be seen reproducibly in 10% of the pads examined (one must find regions that are defect-free), but repeated cycling decreases the rectification ratio, as the molecules must reorient in the intense electrical fields. Temperature-dependent studies are in progress.

Table 1. Estimates of the Energy Level E_{LUMO} for **5** (Relative to the Vacuum Level, Using the Work Functions of M_2) That Must Be Populated before Significant Through-Molecule Tunneling Can Occur (Eqs 20 and 21)[a]

	LB layers	M_2	ϕ_2 (eV)	M_1 (V)	$\lvert\Delta V\rvert$ (eV)	E_{LUMO}
Figure 7	4	Al	4.2	Al	1.0	3.2
Figure 8	4	Mg	3.7	Al	1.0	2.7
Figure 9	1	Al	4.2	Al	1.5	2.8
Figure 11a	1	Al	4.2	Al	1.3	2.9
Figure 14	15	HOPG	4.4	Pt	1.2	3.2

[a] The average is $E_{LUMO} = 3.0 \pm 0.3$ eV.

We have confirmed that **5** is not only a multilayer rectifier but also a monolayer rectifier, by an improvement of Sambles and co-workers' original technique[27,28] and in accord with a plausible modification of the Aviram−Ratner ansatz.[17] We have eliminated the uncertainty due to the previous use[27,28] of two dissimilar metal electrodes with different work functions (Mg and Al).

The work functions ϕ of the relevant metals are 5.7 eV for Pt, 4.4 eV for graphite, 4.2 eV for Al, and 3.7 eV for Mg. We have several measures for the bias ΔV required for the onset of asymmetric conduction through LB monolayers and multilayers of **5**:

(a) through 4 monolayers sandwiched between Al and Al: $\Delta V \approx 1$ V (Figure 7);

(b) through 4 monolayers between Mg and Al: $\Delta V \approx 1$ V (Figure 8);

(c) through 1 monolayer between Al and Al: $\Delta V \approx 1.5$ V (Figure 9);

(d) through 1 monolayer between Al and Al: $\Delta V \approx 1.3$ V (Figure11a);

(e) through 15 monolayers between HOPG and Pt: $\Delta V \approx -1.2$ V (Figure 14).

Using the metal work functions as references, these data yield several estimates of the excited state molecular energy level E_{LUMO} that must be reached before the onset of down-hill intramolecular tunneling (Figure 19 and Table 1); the average is $E_{LUMO} = 3.0 \pm 0.3$ eV.

The experimental electron affinity of TCNQ, **2**, is 3.3 ± 0.3 eV:[46] the through-film conductivity data (Figures 7, 8, 9, 11a and 14) suggest that molecule **5** is a poorer acceptor than TCNQ by 0.3 eV in the gas phase; this agrees approximately with the CV data (Figure 2), which show that **5** is more difficult to reduce than TCNQ by 0.7 V in CH_2Cl_2 solution. The optical band centered at 570 nm (Figure 5) provides an estimate of $\Delta E = E_{LUMO} - E_{HOMO} = 2.17$ eV for the energy gap; this suggests $E_{HOMO} = 5.2$ eV below the vacuum level.

Published PM3 semiempirical calculations for **5**,[30] and the ones presented here, give lower ground-state dipole moments than experiment: the geometry-optimized molecule is less polar, and its bond lengths are quinonoid rather than benzenoid. A very twisted zwitterion with high dipole moment is obtained for the PM3 excited singlet state of **5**. For a shorter alkyl chain, AM1 calculations yield a lower dipole moment for the excited singlet than for the ground state.[44] High calculated dipole moments can be obtained when the Hamiltonian is modified to model the presence of a solvent, both for the ground state[30] and also for the excited singlet state. A large change in dipole moments between the ground and the optically excited state is expected from the large second-order optical nonlinearity of **5**, but is not found easily in the theoretical calculations.

The theoretical (PM3) estimates $E_{HOMO} = -7.98$ eV and $E_{LUMO} = -2.42$ eV yield $\Delta E = 5.56$ eV, a very high result, affected by the usual errors in using Koopmans' theorem. Using the differences in the AM1-computed enthalpies of formation

for the ground-state singlet and the excited singlet (of a modification of **5** with an octyl chain instead of a hexadecyl chain), we estimate $\Delta E = 3.21$ eV, which is closer to experiment. Thus, for an isolated molecule **5**, the D$-\pi-$A state may lie about 3.2 eV above the $D^+-\pi-A^-$ state.

We have improved on the initial claim of rectification by monolayers[27] and multilayers of **5**[28] by showing that even a single monolayer of **5**, can rectify when sandwiched between two electrodes of the same metal (Al, plus its inevitable covering of oxide).

We have detected asymmetric electron flow through a single monolayer, and demonstrated that electrical rectification involves the molecular energy levels of **5**, as expected in a suitable modification of the Aviram−Ratner mechanism.

17. Conclusions

We have proved that a monolayer of molecule **5** can rectify by intramolecular tunneling, and that monolayers and multilayers rectify both as macroscopic films (Figures 7, 8, 9 and 11) and on a nanoscopic level (Figures 14 and 17).

Acknowledgment. We are grateful to Prof. J. Roy Sambles (U. Exeter) for many discussions, to the National Science Foundation (Grant DMR-94-20699), to the Department of Energy (Grant DE-FC02-91-ER-75678), to the Department of Energy for a Predoctoral Traineeship (X.W.), and to the Scientific Affairs Division of the North Atlantic Treaty Organization (Grant CRG 960656) for their support.

Note Added in Proof: Two articles have been brought to our attention: resonant tunneling through a porphyrin (Tao, N. J. *Phys. Rev. Lett.* **1996**, *76*, 4066−4069) and asymmetric tunneling through halogen adatoms on Ag (Schott, J. H.; White, H. S. *J. Phys. Chem.* **1994**, *98*, 297−302). Also, since a 4.5 mm^2 Al pad, covering a monolayer of **5** (area $\approx$ 60 $Å^2$ $molecule^{-1}$), generates a current of 0.0004 mA at $\approx$ 1.5 V (Figure 11a), therefore, one can estimate the electron transfer rate as $k_{ET} = 4.0 \times 10^{-7}$ C pad^{-1} s^{-1}/(1.6×10^{-19} C $electron^{-1}$ $\times$ 4.5×10^{-2} cm^2 pad^{-1}/6.0×10^{-15} cm^2 $molecule^{-1}$) = 0.33 electrons $molecule^{-1}$ s^{-1}.

JA971811E